

Research Article

Kunanon Sakkampang, Chatcharin Sakkampang*, and Davika Sakkampang

An experimental study and finite element analysis of the parametric of circular honeycomb core

<https://doi.org/10.1515/jmbm-2022-0011>

Received Jan 03, 2022; accepted Mar 19, 2022

Abstract: This paper experimentally and numerically investigated the impact test response and characteristics of circular honeycomb cores. The experiments were conducted on two different structures of aluminum-tube honeycomb core, square structure and star structure. The specimens were tested in order to find energy absorption, specific energy absorption, and crashworthiness behaviors. The results revealed that circular honeycomb cores with star structure could resist higher impact load than circular honeycomb cores with square structure. In addition, the larger tubes showed a lower impact load the smaller tubes. It was also revealed that the greater the collapse distance of the aluminum-tube honeycomb core, the lower the load. Moreover, FEA simulation results, through ABAQUS.CAE, were compared to the experimental results. The results revealed that good agreement was achieved between the experimental results and the FEA results. The comparison results showed that the difference in maximum load between experimental and FEA model was 0.47–11.84%, which is a reliable analysis result. In terms of energy absorption and specific energy absorption, the difference in maximum load between experimental and FEA model was 23.54% and 16.23%, respectively.

Keywords: circular honeycomb core, energy absorption, specific energy absorption

1 Introduction

Nowadays in the material industry, the focus is on lightweight but high energy absorbing materials or structures with low density and high mechanical efficiency, such as [1] foams [2], honeycomb materials [3, 4], wood core [5–7] and lattice materials [8]. Aluminum is especially widely used in the aerospace industry due to its light weight, high strength and stiffness [9]. Aluminum tubes are widely used in automotive applications, sea freight and other engineering fields. The advantages of aluminum tubes are specific strength and high energy absorption capability, good crashworthiness and impact applications [10]. In the past, there has been extensive research on thin-walled structures from experiments [11, 12], theoretical analysis [13, 14] and model analysis [15, 16]. The shape structure of aluminum tubes with different cross-sectional shapes has become an important area of research, including circular [17, 18], square [13], polygonal [19] and multi-cell pipe [20]. Analysis of the shape of the aluminum honeycomb material is an interesting topic to study because the aluminum honeycomb material is lightweight and has a high strength-to-weight ratio. Their good compressive properties make them suitable for absorbing energy [21–23]. It has good shock absorbing ability and a wide application in both the shock absorbing and the automotive industries.

Aluminum honeycomb has been widely investigated theoretically, numerically and experimentally [24]. Most of these studies are focused on hexagonal honeycomb aluminum sheet such as, in-plane and off-plane mechanical behavior of honeycomb structures under quasi-static and dynamic compression [25, 26]. Thomas and Tiwari [27] examined the strengthening behavior of aluminum honeycomb and found that the solidification of the honeycomb structure during dynamic loading was mainly due to the pressure changes caused by air confined within the cavity of a part of the beehive. Balaji and Annamalai [28] and Sun *et al.* [29] examined the effect of foil thickness and cell size of honeycomb aluminum on the impact behavior of aluminum honeycomb panels. Palomba *et al.* [30] examined the low-velocity impact behavior of aluminum honeycomb panels taking into account the effect of honeycomb cell

***Corresponding Author: Chatcharin Sakkampang:** Department of Mechanical Engineering, Faculty of Engineering, Rajamangala University of Technology Isan Khon Kaen Campus, Thailand; Email: chatcharin.sk@rmu.ac.th

Kunanon Sakkampang: Department of Mechanical Engineering, Faculty of Industry and Technology, Rajamangala University of Technology Isan Sakon Nakhon Campus, Thailand

Davika Sakkampang: Department of Liberal Art, Faculty of Industry and Technology, Rajamangala University of Technology Isan Sakon Nakhon Campus, Thailand

size, and cell pattern on the behavior of shock. Several studies have shown that low-velocity shock behavior is highly dependent on cell size [31] and that cell pattern and size have a significant effect on loading. The impact of size and form on aluminum honeycomb is substantial and will likely guide future studies. Finite element analysis (FEA) which has been widely publicized is used in analyses [32, 33] and shows a significant advantage in characterizing an initial damage behavior [34]. For example, Zhang *et al.* [35] investigated the effects of dynamic shock response and the characteristics of a foam-filled aluminum honeycomb (Expanded Polypropylene) experimentally and numerically. It was found that the strength and the average strength of the honeycomb were increased but the specific energy absorption was decreased. In addition, the model analysis survey revealed that the model was able to accurately analyze the results and compared it to the experimental results. Zhou *et al.* [36] also studied the strength test of concrete reinforced with aluminum honeycomb. It was found that the off-plane strength and energy absorption capacity of the honeycomb of the same areal density increased with a 33–207% increase in cell size compared to conventional concrete, as demonstrated by the model which was able to analyze the results with the same accuracy compared to the experiment. Balaji and Annamalai [28] conducted an experimental evaluation and simulation analysis of hollow rectangular aluminum columns filled with carbon

fiber and aluminum honeycomb at a constant speed of 3.06 mm/s. Numerical simulations performed using the finite element method showed a clearer effect of specific energy absorption and maximum pressure efficiency increase by 60.6%, 27.8% and 17.4%, respectively. FEA methodological study showed that the program was able to analyze the constituent correlations for studying the crushing behavior of honeycombs under complex load conditions [37] which was a necessary addition to develop future models. With an increasing demand on energy absorption capacity in cushioning material, scholars have been trying to find and develop novel honeycomb structures with new geometric configuration [38].

The above studies show that aluminum is considered to be a material with good impact strength and energy absorption [39–42]. However, previous studies have mainly focused on the effects of octagonal honeycomb cores with star structure [3, 4, 9, 10, 16], thus, this study aims to examine the effect of circular honeycomb cores with different diameters and arrangement. The circular honeycomb cores were selected in this study because they were easy to fabricate from round pipes. An impact test and an impact behavior study using a finite element analysis program were used to verify the results. This study might be useful as a guideline for designing circular pipe into suitable size to make a honeycomb sheet for absorbing impact in the future.

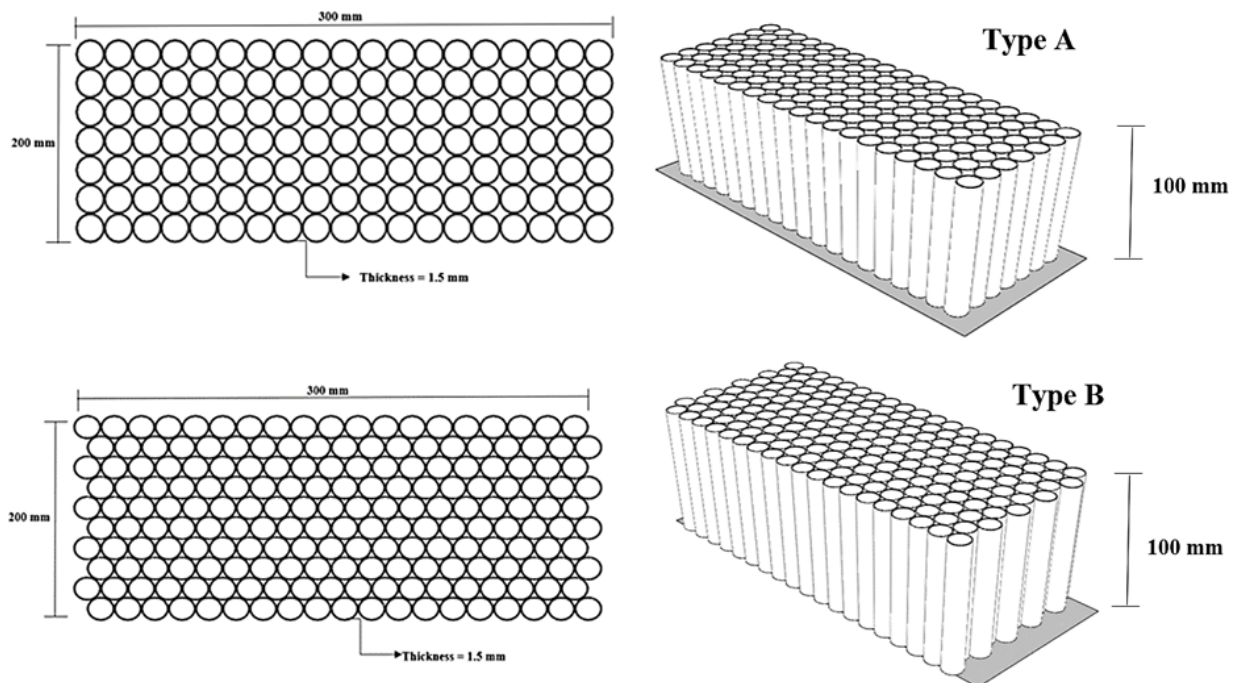
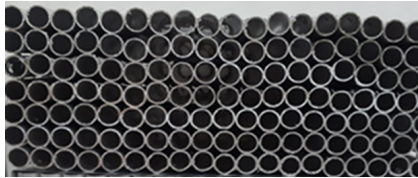
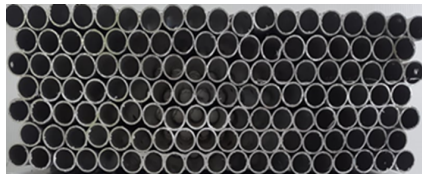
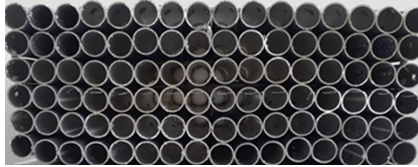
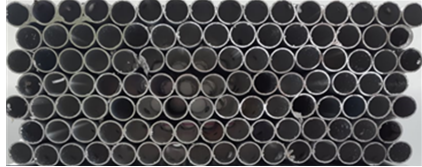




Figure 1: The width, length, height and thickness of circular honeycomb Core with square structure (Type A) and circular honeycomb Core with star structure (Type B)

Table 1: Characteristics of circular honeycomb core with square structure (Type A) and circular honeycomb core with star structure (Type B)

DIMETER OF TUBE (INCH)	TYPE A	TYPE B
12 MM. (TYPE A1 AND TYPE B1)		
15 MM. (TYPE A2 AND TYPE B2)		
25 MM. (TYPE A3 AND TYPE B3)		

2 Methodology

2.1 Specimens

To study the shock absorption of grade 6061 round aluminum tubes, three tube sizes were selected in this experiment, 12 mm, 15 mm and 25 mm with the thickness of 1.5 mm. The dimension of the specimen had specified width \times length of the panel at 200×300 mm and was divided into 2 types of pipe structures: square structure (Type A) and star structure (Type B). The aluminum pipe was cut into 100 mm long. The cut tubes were welded together and arranged in a row in a bee retaining style, as shown in Table 1. In this research, the size of the honeycomb sheet was divided into 6 types as seen in Table 1.

2.2 Impact testing machine

In this research, the specimens were freely dropped from impact testing machine where a load cell was installed as in Onsalung *et al.* [43], Junchuan and Thinvongpituk [44] and Sakkampang and Thinvongpituk [45]. The aluminum honeycomb tube is quite hard; therefore, this research used a 30-kg hammer head with 15-cm diameter. To test the load, a 4-metre impact testing machine with a pulley set to pull the hammer head up to the specified height was used as shown in Figure 2. The impact heights were tested at 2 m (V

= 6.26 m/s), 3 m ($V = 7.67$ m/s), and 4 m ($V = 8.68$ m/s). The experiment involved dropping a hammer head against the specimens with a 50 kN dynamic load cell at the base of the specimen. A data logger was used to analyze the data dynamically using GREENTECH GTDL-350 brand logger which can record data at a frequency of up to 10,000 values per second. When shock was applied to the load cell, the load cell recorded the resulting load and converted it to electrical signals through the data logger. The load transmitted the data to the computer in kN.

The result of the load generated by the computer was expressed as the relationship between load and time (ms). When the result of the load was applied, the average load (P_{mean}) was calculated to calculate the energy absorption as shown in Eq. (1) [46]. The collapse distance of the specimen after impact was measured to determine the specific energy absorption, which is defined as the energy absorption of a particular structure compared to the weight of the structure itself. The specific energy absorption resulting from the impact was determined using Eq. (2) [47].

$$E_a = P_{mean} \cdot S \quad (1)$$

where E_a is the energy absorbed by the workpiece, P_{mean} is the load acting on the workpiece, S is the distance the workpiece material collapses from start to finish.

$$E_s = \frac{\int PdS}{mass} \approx \frac{P_{mean} \cdot S}{mass} \quad (2)$$

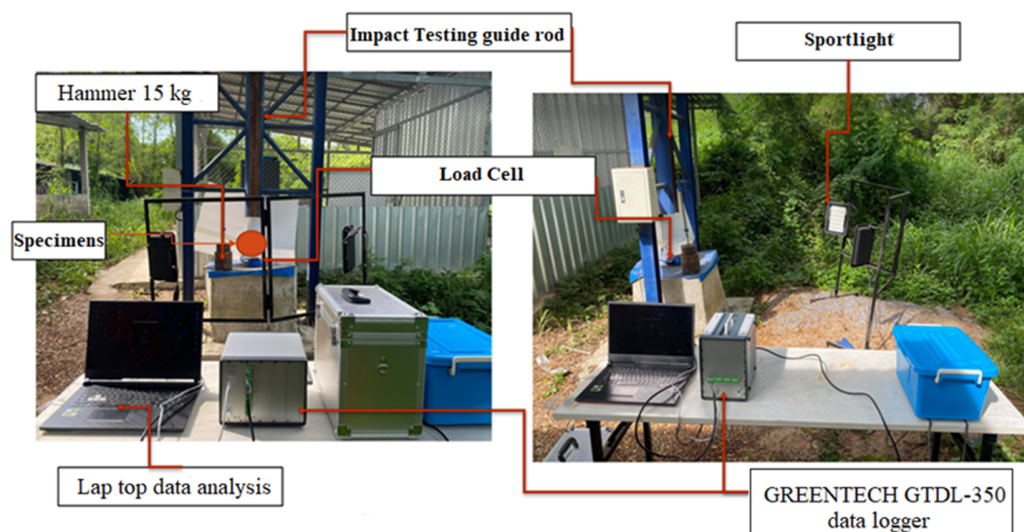


Figure 2: Impact testing machine used in this study *spotlight, laptop

where E_s is the specific energy absorption, mass is the mass of the workpiece, P_{mean} is the average load.

2.3 Material properties and finite element analysis (FEA)

In this study, 3 models which consisted of hammer head, aluminum honeycomb tubes, and square steel plates were used to store load data. ABAQUS.CAE program was used to analyze the model by defining the hammer head and steel plate as a discrete rigid, while the aluminum honeycomb tube was determined as a deformable material. Poisson's ratio was taken from Onsalung *et al.* [43]. Young's modulus and Maximum yield strength derived from tensile test. The properties of aluminum tubes can be seen in Table 2.

Table 2: Aluminum properties used in FEA

Properties	Description	Value
ρ	Density (kg/m^3)	2,700
E	Young's modulus (GPa)	40
ν_{12}	Poisson's ratio	0.33
σ	Maximum yield strength (MPa)	190

When the material properties are defined, then the conditions for model analysis are determined. The condition of the analysis was defined as Dynamic/Explicit by requiring that the hammer head, which was defined as a solid (3D - Discrete Rigid), fell in the Y axis (Free U2) with a weight of 30 kg, hitting the aluminum honeycomb round tube as

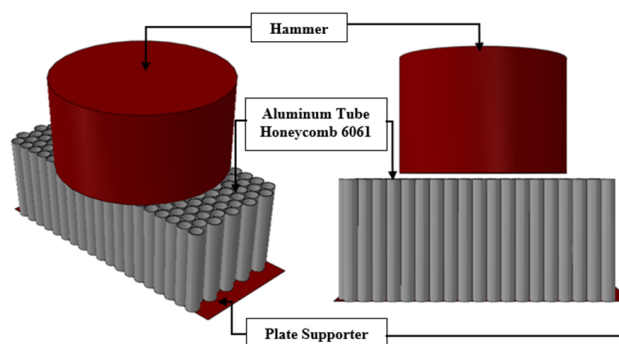


Figure 3: Characteristics of model analysis of aluminum honeycomb sheet in ABAQUS.CAE program

the 3D – deformable material. The aluminum honeycomb sheet at the base was a solid steel sheet (3D - Discrete Rigid) was used to support the aluminum honeycomb body as shown in Figure 3. This steel plate determined the nature of the plate's motion without any movement ($U_1, U_3, UR_1, UR_2, UR_3 = 0$). The coefficient of friction of the workpiece contact surface was determined to be 0.15 and the effect of the impact load on the steel plate adjacent to the aluminum honeycomb was stored at point (RF1) as shown in Figure 4. This was consistent with the practice of laboratory testing, where the load cell to store the load data is placed below the specimen in the experiment. The mesh definition and mesh size of the material in the model are defined as a 10 mm A 4-node 3-D bilinear rigid quadrilateral (R3D4) mesh. The mesh convergence was not conducted since the material was rigid quadrilateral. In the case of aluminum honeycomb which is defined as 3D - Deformable, the mesh pattern is defined as a 10-node modified quadratic tetrahedron (C3D10M), and mesh size was used at 1 mm.

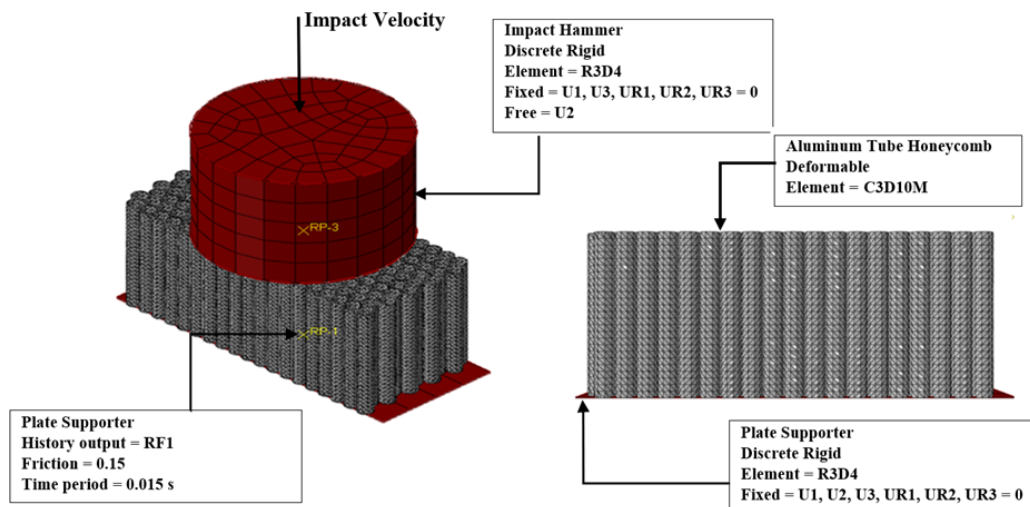


Figure 4: Mesh determination and model analysis conditions of aluminum honeycomb material

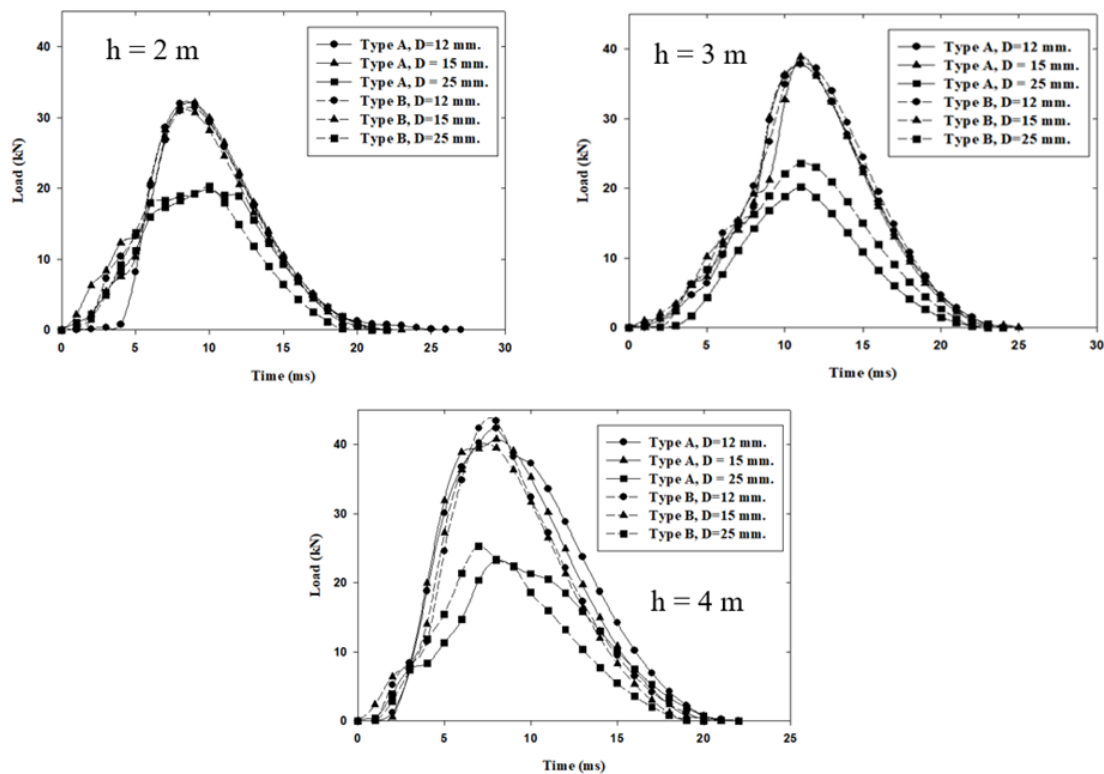


Figure 5: The impact load of Type A and Type B

3 Results and discussion

3.1 Energy absorption and crashworthiness behaviors

The impact load of the circular honeycomb cores with the diameter of 12 mm, 15 mm, and 25 mm was studied at an impact height of 2-4 m. The first step was to perform impact

load analysis. The average load and collapse distance of the circular honeycomb cores before the energy absorption and specific energy absorption were calculated. In case of Type A as shown in Figure 5, it was found that model A1 had a maximum load of 32.01, 37.82 and 42.33 kN at 2, 3 and 4 m, respectively, while model A3 had the maximum load of 19.82, 20.17 and 23.22 kN at 2, 3 and 4 m, respectively, which was found to be consistent with Type B specimens

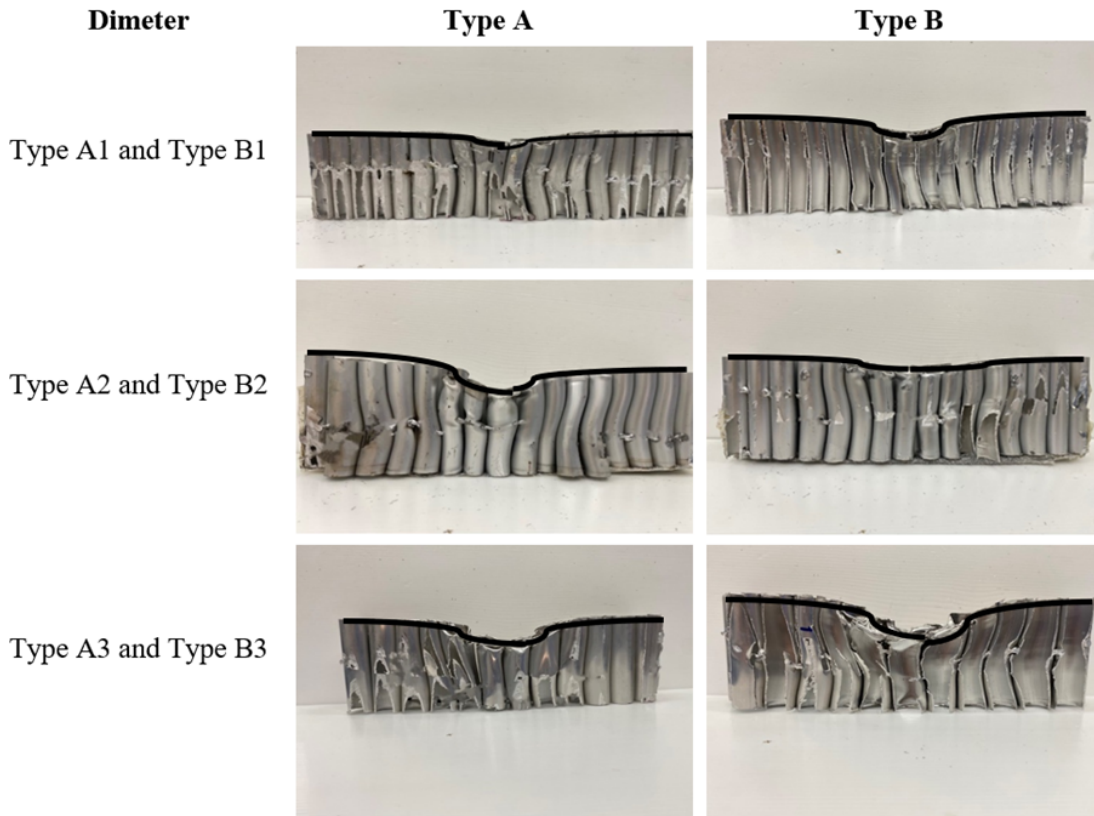


Figure 6: Collapse patterns of Type A and Type B at a height of 4 m

Table 3: Results of P_{max} , P_{mean} , and displacement (S) of experimental and FEA

<i>Dimeter</i>	<i>h</i> (m)	$P_{max}(kN)$ <i>Exp.</i>	$P_{max}(kN)$ <i>Sim.</i>	<i>Diff</i> (%)	$P_{mean}(kN)$ <i>Exp.</i>	$P_{mean}(kN)$ <i>Sim.</i>	<i>S</i> (m) <i>Exp.</i>	<i>S</i> (m) <i>Sim.</i>
Type A1	2	32.01	36.14	11.43	10.38	14.3	0.009	0.009
	3	37.82	37.10	1.90	13.02	13.55	0.009	0.01
	4	42.33	38.73	8.50	17.23	17.85	0.011	0.011
Type A2	2	32.07	31.02	3.27	11.64	14.38	0.008	0.009
	3	37.90	37.22	1.79	13.55	14.99	0.009	0.009
	4	39.44	36.78	6.74	16.9	15.33	0.011	0.012
Type A3	2	19.82	20.88	5.08	10.01	11.02	0.013	0.015
	3	20.17	21.94	8.07	6.6	8.37	0.019	0.017
	4	23.22	23.58	1.53	9.99	10.22	0.021	0.023
Type B1	2	33.41	35.24	5.19	11.98	14.56	0.004	0.007
	3	37.93	38.69	1.96	13.59	13.62	0.006	0.008
	4	43.44	45.48	4.49	18.87	19.33	0.009	0.009
Type B2	2	32.08	32.99	2.76	12.54	12.48	0.005	0.009
	3	37.91	38.09	0.47	14.31	14.94	0.008	0.009
	4	39.95	38.19	4.41	16.79	16.6	0.010	0.011
Type B3	2	20.33	23.06	11.84	9.03	9.59	0.011	0.013
	3	23.59	23.96	1.54	9.13	9.05	0.012	0.018
	4	25.29	25.78	1.90	10.14	10.14	0.017	0.019

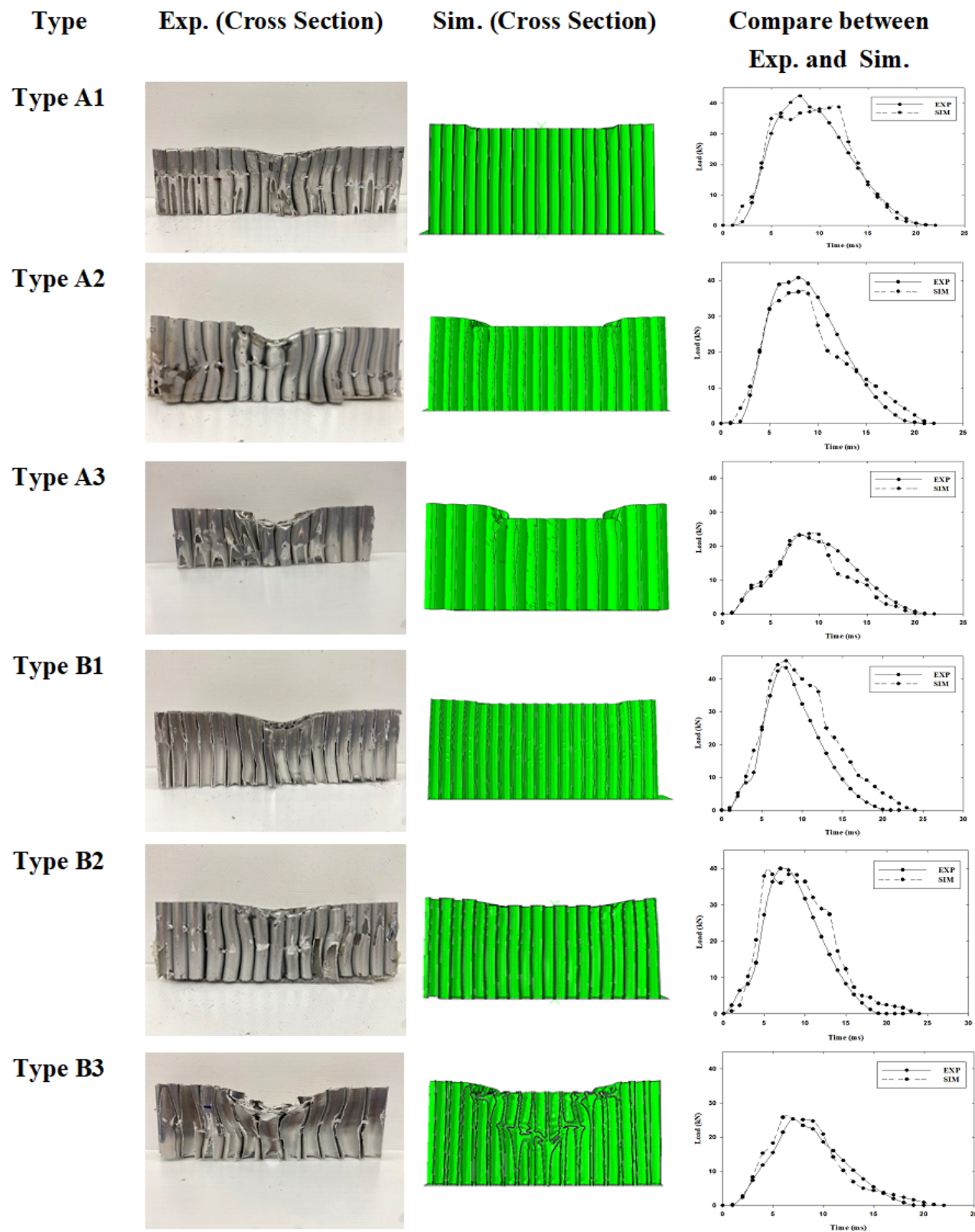


Figure 7: Crashworthiness patterns of circular aluminum honeycomb Type A and Type B at 4 m height by comparison of experimental and FEA simulation analysis

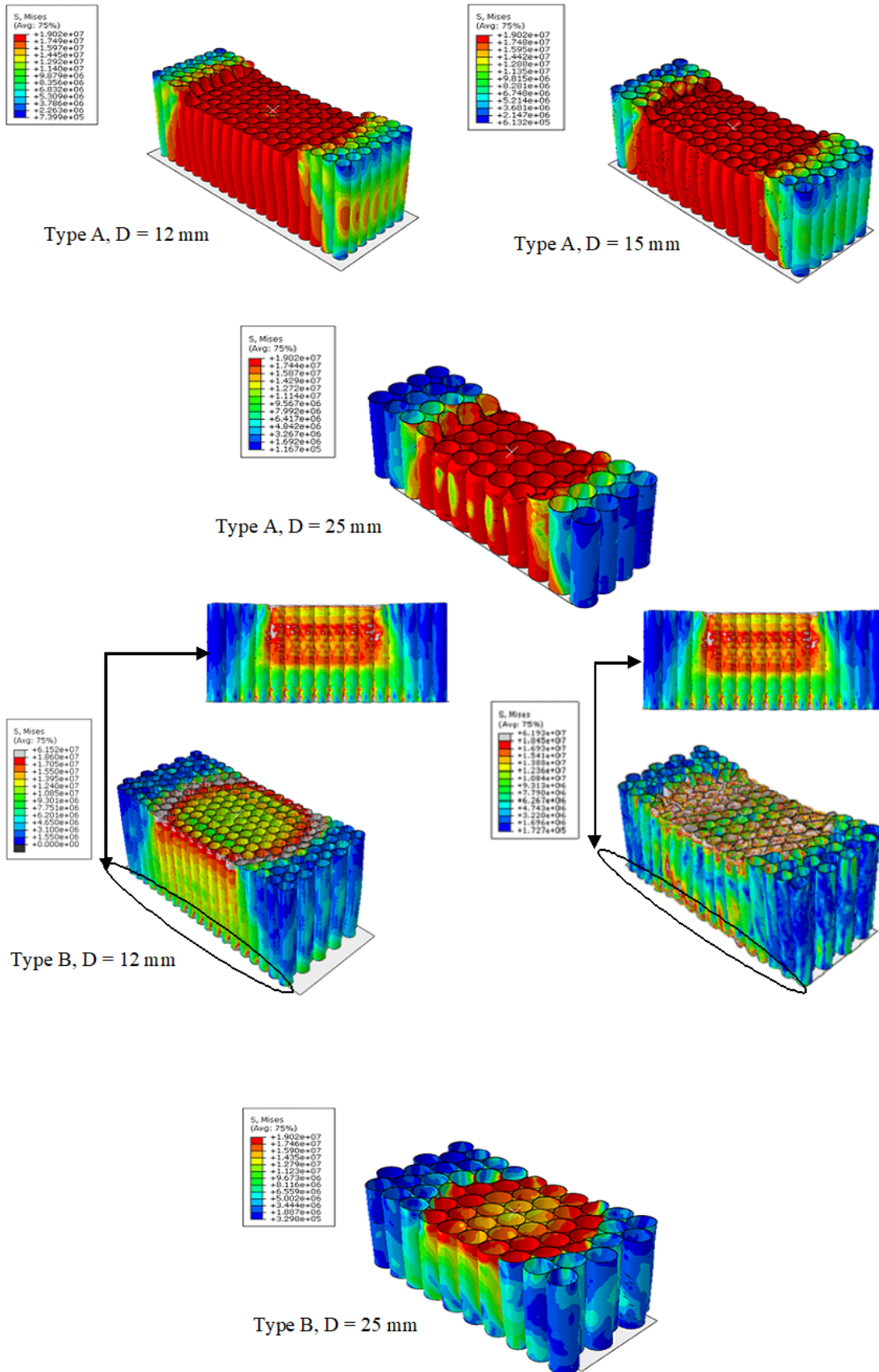


Figure 8: Characteristics of crashworthiness of circular aluminum honeycomb Type A and Type B at 4 m height by FEA model analysis

in that the specimens with larger diameter tubes had lower maximum load. However, it was noted that Type A had better load absorption capacity. This showed that the pattern of tube arrangement affected the impact strength, with the straight-tube arrangement having better impact resistance than the star-tube arrangement.

The collapse characteristics of the specimens at a height of 4 m ($V = 8.68$ m/s), the highest height, are shown in Figure 6. It was found that the collapse characteristics of the aluminum-tube honeycomb core of both Type A and Type B were similar in that the tubes with larger diameters had more collapse than tubes of smaller diameters. The collapse distances of models A3 and B3 were 0.021 and 0.017 m at a height of 4 meters. In the experiments, some errors occurred because the welded joints on the specimens was at a single point, but in the FEA analysis, the welded joints were seen along the tubes. The average load and collapse distance of the specimen at all heights can be seen in Table 3.

3.2 Comparison of experimental results and model analysis by FEA

To compare the collapse patterns of the experimental results and FEA results, the model of 4 m was discussed as an example. The cross section is presented in Figure 7. Considering the graph characteristics showed that the graph is mountain-shaped graph which was relevant to the study of Zhang *et al.* [46] and Pratomo [47]. The damage and collapse were similar in Models A1 and B1. As for the load, it was found that Type B had a slightly higher peak load than Type A. The maximum load of Type A was 42.33 kN, while that of Type B was 43.44 kN. Similarly, it was found that the larger diameter tubes were able to absorb the load better than the smaller diameter tubes which was consistent with the study of Hao and Du [48] and Z. Dong *et al.* [49]. The effect of the maximum load can be seen in Table 3.

By comparing the results of the experiments and the results of the model analysis, it was possible to analyze whether the experimental and model values had a good agreement. The difference P_{max} between the experimental results and the model results was 1.53–11.84% at the test at 4 m, which is similar to 2 and 3 m height tests. The results of the model analysis showed that the greater the collapse distance of the aluminum-tube honeycomb core, the lower the load. This may affect the analysis in terms of energy absorption and specific energy absorption. Table 3 shows the collapse distance of the specimens in all cases which is considered important for the calculations in equations 1 and 2.

Figure 8 shows distribution of von Mises stress of type A and type B model at the height of 4 m. Type A pattern showed the hammer head impact as being centered with more collapse than Type B and the distribution of the transmitted force was better than Type B. The von Mises stress of Type A was 19.02 MPa for most of the core area. The von Mises stress of Type B was 61.52 MPa in some areas, particularly on the hammer-head side and the bottom of the tubes where the transmission of stress results in the load was higher than Type A. However, it could be seen that the model B3 tended to have a von Mises stress distribution similar to that of the von Mises stress distribution of model A3. The difference is that the collapse distance of type B was less than types A hence that caused a higher load characteristics. From the FEA model analysis results in Figure 8, the tendency of the von Mises stress distribution can be seen. Type A had a better force distribution than Type B which had a greater transmission to the bottom or storage point than Type A. This was the same as the FEA of heights at 2 and 3 m, respectively.

3.3 Energy absorption and specific energy absorption

Figure 9 shows the energy absorption. It was found that energy absorption of Type A and Type B was similar with Type A being slightly more energy-absorbing than Type B. The size of the aluminum tube consideration showed that the energy absorption of model A3 at the height of 4 m was $E_a = 0.2098$ kN.m and while that of model B3 was $E_a = 0.1724$ kN.m. From the experimental results on the size of the aluminum tubes, it was found that the larger tubes had the ability to absorb more energy than the smaller tubes which was in line with the results of the experiments of Xie and Zhou [50] where the graph was similar at all impact heights. This was consistent with the results of the FEA model analysis which revealed that larger tubes had more collapse than smaller tubes, resulting in higher energy absorption than smaller tubes. The largest percentage difference between the experimental results and the FEA analysis was found to be 44.17% in model B2, while the closest value was model B1 with a difference of 2.41%. The percentage difference of experimental and FEA model analysis can be seen in Table 4.

Table 4 shows the specific energy absorption. It can be seen that the specific energy absorption values depended mainly on the energy absorption values. If the energy absorption is high, the specific energy absorption will also be high. The highest specific energy absorption values were found in model A3. The experimental and model analysis

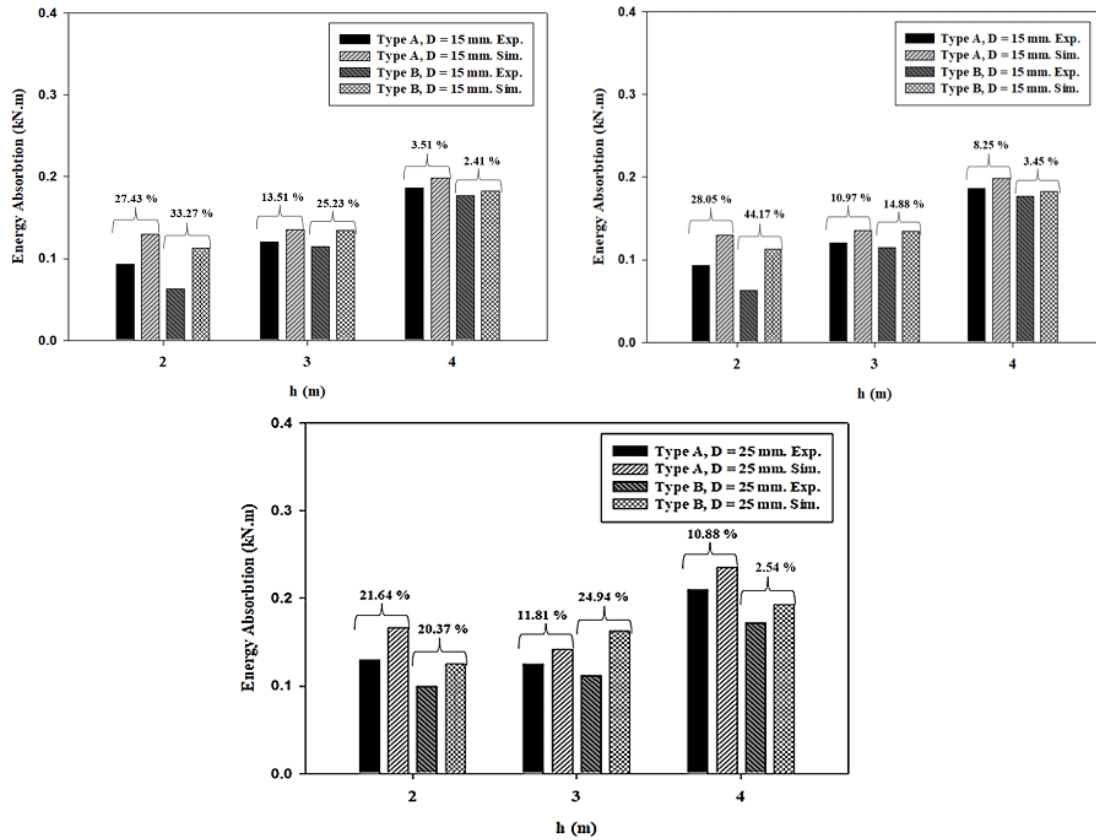


Figure 9: Results of experimental and FEA model analysis of energy absorption of circular aluminum honeycomb Type A and Type B

Table 4: Differences between the experimental and FEA model analyzes of the energy absorption of Type A and Type B circular aluminum honeycomb

Dimeter	h (m)	E_a (kN.m) Exp.	E_a (kN.m) Sim.	Diff (%)	E_s (kN.m/kg) Exp.	E_s (kN.m/kg) Sim.	Diff (%)
Type A1	2	0.0934	0.1287	27.43	0.0577	0.0794	7.94
	3	0.1172	0.1355	13.51	0.0723	0.0836	8.36
	4	0.1895	0.1964	3.51	0.1170	0.1212	12.12
Type A2	2	0.0931	0.1294	28.05	0.0621	0.0863	8.63
	3	0.1201	0.1349	10.97	0.0801	0.0899	8.99
	4	0.1859	0.1983	6.25	0.1239	0.1322	13.22
Type A3	2	0.1300	0.1659	21.64	0.0897	0.1144	11.44
	3	0.1254	0.1422	11.81	0.0865	0.0981	9.81
	4	0.2098	0.2354	10.88	0.1447	0.1623	16.23
Type B1	2	0.0679	0.1019	33.37	0.0296	0.0629	6.29
	3	0.0815	0.1090	25.23	0.0503	0.0673	6.73
	4	0.1698	0.1740	2.41	0.1048	0.1074	10.74
Type B2	2	0.0627	0.1123	44.17	0.0418	0.0749	7.49
	3	0.1144	0.1344	14.88	0.0763	0.0896	8.96
	4	0.1763	0.1826	3.45	0.1175	0.1217	12.17
Type B3	2	0.0993	0.1247	20.37	0.0685	0.0860	8.60
	3	0.1222	0.1628	24.94	0.0774	0.1123	11.23
	4	0.1878	0.1927	2.54	0.1189	0.1329	13.29

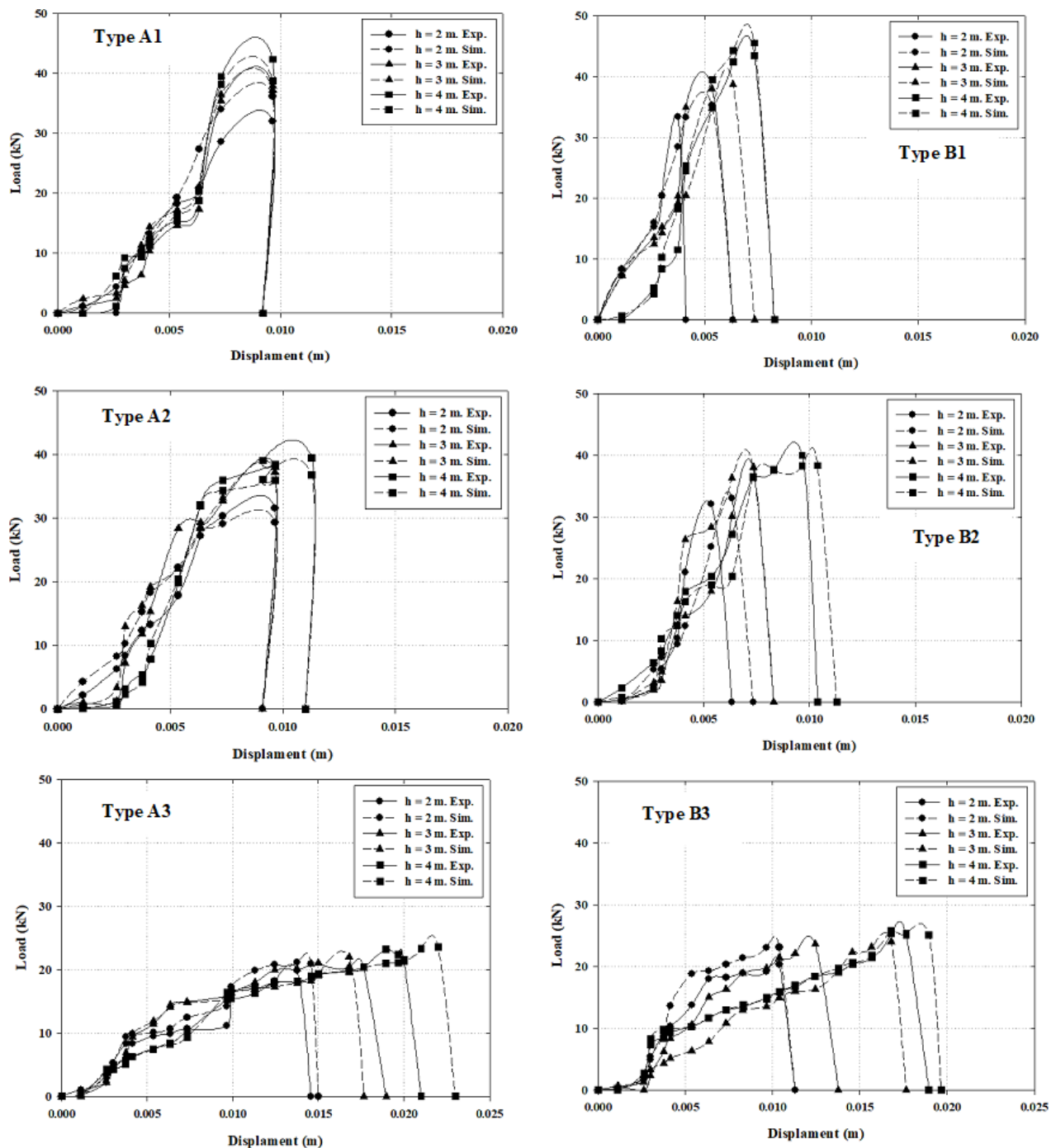


Figure 10: Comparative results between the collapse displacement and load of Type A and Type B

results were 0.1447 and 0.1623 kN.m/kg, respectively, with the percentage difference between the experimental and simulation results at 16.23%. It was found that smaller tubes had a lower specific energy absorption capacity than larger tubes. The tube structures Type A and Type B had similar tendencies. Figure 10 shows the specific energy absorption capacity of each tube size at different test heights. When analyzing both the experimental results and the FEA, it was

found that the obtained values were consistent. Considering the analysis of research by Zhang *et al.* [51], it was found that the greater the deflection of a material, the higher the energy absorption and specific energy absorption effect. Experimental and simulated analyzes have also shown that the greater the bending, deflection, or collapse of a material, the higher the energy absorption and specific energy absorption.

3.4 The relationship between displacement and load

Figure 10 shows the results of the comparison between the collapse displacement of the specimen and the impact load which revealed that higher load led to higher collapse displacement of the specimens. This was consistent with the research of Zhang *et al.* [46] and Qi *et al.* [52]. The collapse behavior showed very high collapse in models A3 and B3, with a collapse distance of up to 0.021 m while models A1, A2, B1, B2 had a collapse value of between 0.004 – 0.011 m. Therefore, as a result of the energy absorption efficiency relation to the impact load, the energy absorption efficiency of Type A3 and Type B3 was significantly better than that of other models. The results of the FEA model analysis also confirmed that the experiments were valid. The larger tubes had a greater collapse characteristic. However, the use of the experimental results in industrial applications should be considered for applications where high strength is required. Tubes with small diameter are probably suitable for high load applications.

4 Conclusion

This paper investigated the effect of different structures of aluminum tubes on the energy absorption and collapse characteristics of circular honeycomb core. FEA simulation by ABAQUS® was also used for detailed investigation and compared to experimental results. The results of this study revealed that the diameter of the aluminum tubes affected the impact load of the specimens. The larger tubes showed a lower impact load than the smaller tubes. However, the different structures of the circular honeycomb core also showed a different result. The specimens with star structure showed a slightly higher performance than the specimens with square structure which led to good energy absorption of the material.

The results of model studies by FEA showed that the difference in maximum load between experiment and FEA model was 0.47–11.84%, which was a reliable analysis result. In terms of energy absorption and specific energy absorption, the difference in maximum load between experimental results and FEA model was 23.54% and 16.23%, respectively.

The energy absorption of Type A3 and B3 were 0.2098 kN.m and $E_a = 0.1878$ kN.m, respectively, which was slightly different at the height of 4 m. The difference in maximum energy absorption between experimental results and FEA model was 10.88% which was considered satisfactory. This

was consistent with the results of the specific energy absorption analysis of Type A3. The results of the experiment and FEA analysis were 0.1447 and 0.1623 kN.m/kg, respectively, with difference percentage of 16.23%. According to the experiments and FEA analysis, it was found that the more the material collapsed, the higher the energy absorption and specific energy absorption. Based on the observation of the collapse behavior of Type A and Type B, it was found that Type A3 showed a collapse distance of up to 0.021 m, which led to good energy adsorption.

As a result of both experimental and analysis by the FEA program, it can be applied in the development of spherical impact materials with a better edge than honeycomb geometry, in terms of materialization and formulation, than octagonal honeycomb course. Its shock-absorbing and energy-absorbing performance is similar to that of the current popular octagonal aluminum honeycomb panels. In future analysis, the impact strength of round aluminum tubes with vertical axis will be studied in order to see the definite experimental results in their application as a load-bearing material.

Acknowledgement: I would like to thank Mr. Weerapan Sakkampang and Mrs. Wanwipa Sakampang for the mental and financial support throughout this research.

Funding information: The authors state no funding involved.

Author contributions: All authors have accepted responsibility for the entire content of this manuscript and approved its submission.

Conflict of interest: The authors state no conflict of interest.

References

- [1] Zhou H, Zhang X, Wang X, Wang Y, Zhao T. Response of foam concrete-filled aluminum honeycombs subject to quasistatic and dynamic compression. *Compos Struct.* 2020;239:112025.
- [2] Chen J, Zhu L, Fang H, Han J, Huo R, Wu P. Study on the low-velocity impact response of foam-filled multi-cavity composite panels. *Thin-walled Struct.* 2022;173:108953.
- [3] Yoon S, Schiffer A, Cantwell WJ, Ki TY. Detection of core-skin disbands in honeycomb composite sandwich structures using highly nonlinear solitary waves. *Compos Struct.* 2021;256:113071.
- [4] Zhou X, Wang L, Yu D, Zhang C. Dynamic effective equivalent stiffness analysis on the periodical honeycomb reinforced composite laminated structure filled with viscoelastic damping material.

- Compos Struct. 2018;193:S0263822317331872.
- [5] Dogan A. Low-velocity impact, bending, and compression response of carbon fiber/epoxy-based sandwich composites with different types of core materials. *J Sandw Struct Mater.* 2021;23(6):1956–71.
 - [6] Ozdemir O, Oztoprak N, Kandas H. Single and repeated impact behaviors of bio-sandwich structures consisting of thermoplastic face sheets and different balsa core thicknesses. *Compos, Part B Eng.* 2018;149:49–57.
 - [7] Dogana A, Arikani V. Low-velocity impact response of E-glass reinforced thermoset and thermoplastic based sandwich composites. *Compos, Part B Eng.* 2017;127:63–9.
 - [8] Nan J, Fuchi W, Yangwei W, Bowen Z, Huanwui C. Effect of structural parameters on mechanical properties of Pyramidal Kagome lattice material under impact loading. *Int J Impact Eng.* 2019;132:103313.
 - [9] Sun M, Wowk D, Mechefske C, Alexander E, Kim IY. Surface and honeycomb core damage in adhesively bonded aluminum sandwich panels subjected to low-velocity impact. *Compos, Part B Eng.* 2022;230:109506.
 - [10] Salem H, Boutchicha D, Boudjemai A. Modal analysis of the multi-shaped coupled honeycomb structures used in satellites structural design [IJIDeM]. *Int J Interact Des Manuf.* 2018;12:955–67.
 - [11] Tak SK, Iqbal MA. Axial compression behaviour of thin-walled metallic tubes under quasi-static and dynamic loading. *Thin-walled Struct.* 2021;159:107261.
 - [12] Padmaja M, Murty VVVS, Ramana Rao NV. Quasi static axial compression of empty and PU foam filled circular aluminium and light gauge square steel tubes. *Mater Today Proc.* 2021;43(2):2342–2347.
 - [13] Xiong MX, Richard Lie JY. Buckling behavior of circular steel tubes infilled with C170/185 ultra-high-strength concrete under fire. *Eng Struct.* 2020;212:110523.
 - [14] Gao Q, Liao WH. Energy absorption of thin walled tube filled with gradient auxetic structures-theory and simulation. *Int J Mech Sci.* 2021;201:106475.
 - [15] Chen H, Zhang Y, Lin J, Zhang F, Wang Y, Yan X. Crushing responses and optimization of novel sandwich columns. *Compos Struct.* 2021;263:113682.
 - [16] Ebrahimi S, Vahdatazad N. Multiobjective optimization and sensitivity analysis of honeycomb sandwich cylindrical columns under axial crushing loads. *Thin-walled Struct.* 2015;88:90–104.
 - [17] Jiao P, Chen Z, Ma H, Ge P, Gu Y, Miao H. Buckling behaviors of thin-walled cylindrical shells under localized axial compression loads, Part 1: experimental study. *Thin-walled Struct.* 2021;166:108118.
 - [18] Zhao X, Liang H, Lu Y, Zhao P. Size effect of square steel tube and sandwiched concrete jacketed circular RC columns under axial compression. *J Construct Steel Res.* 2019;166:105912.
 - [19] Ha NS, Pham TM, Hao H, Lu G. Energy absorption characteristics of bio-inspired hierarchical multi-cell square tubes under axial crushing. *Int J Mech Sci.* 2021;201:106464.
 - [20] Li Z, Ma W, Yao S, Xu P. Crashworthiness performance of corrugation- reinforced multicell tubular structures. *Int J Mech Sci.* 2021;190:106038.
 - [21] Li Z, Sun H, Wang T, Wang L, Su X. Modularizing honeycombs for enhancement of strength and energy absorption. *Compos Struct.* 2022;279:114744.
 - [22] Wang T, Li Z, Wang L, Hulbert GM. Crashworthiness analysis and collaborative optimization design for a novel crash-box with re-entrant auxetic core. *Struct Multidiscipl Optim.* 2020;62(4):2167–79.
 - [23] Li Z, Wang T, Yi J, Wang L, Liu D. Design-oriented crushing analysis of hexagonal honeycomb core under in-plane compression. *Compos Struct.* 2018;187:429–38.
 - [24] Yang X, Sun Y, Yanga J, Pan Q. Out-of-plane crashworthiness analysis of bio-inspired aluminum honeycomb patterned with horseshoe mesostructure. *Thin-walled Struct.* 2018;125:1–11.
 - [25] Li Z, Yang Q, Chen W, Hao H, Fang R, Cui J. Dynamic compressive properties of reinforced and kirigami modified honeycomb in three axial directions. *Thin-walled Struct.* 2022;171:108692.
 - [26] Xie S, Zhou H. Analysis and optimisation of parameters influencing the out of plane energy absorption of an aluminium honeycomb. *Thin-walled Struct.* 2015;89:169–77.
 - [27] Thomas T, Tiwari G. Energy absorption and in-plane crushing behavior of aluminium reinforced honeycomb. *Vacuum.* 2019;166:364–9.
 - [28] Balaji G, Annamalai K. Crushing response of square aluminium column filled with carbon fibre tubes and aluminium honeycomb. *Thin-walled Struct.* 2018;132:667–81.
 - [29] Sun M, Wowk D, Mechefske C, Alexander E, Kim IY. Surface and honeycomb core damage in adhesively bonded aluminum sandwich panels subjected to low-velocity impact. *Compos, Part B Eng.* 2020;230:109506.
 - [30] Palomba G, Crupi V, Epasto G. Collapse modes of aluminium honeycomb sandwich structures under fatigue bending loading. *Thin-walled Struct.* 2019;145:106363.
 - [31] Zhang Y, Zong Z, Liu Q, Ma J, Wu Y, Li Q. Static and dynamic crushing responses of CFRP sandwich panels filled with different reinforced materials. *Mater Des.* 2017;117:396–408.
 - [32] Qin Q, Xia Y, Li L, Chen S, Zhang W, Li K, et al. On dynamic crushing behavior of honeycomb-like hierarchical structures with perforated walls: experimental and numerical investigations. *Int J Impact Eng.* 2020;145:103674.
 - [33] Audibert C, Andréani AS, Lainé E, Grandidier JC. Discrete modelling of low-velocity impact on Nomex® honeycomb sandwich structures with CFRP skins. *Compos Struct.* 2019;207:108–18.
 - [34] Yang B, Wang H, Chen Y, Fu K, Li Y. Experimental evaluation and modelling of drilling responses in CFRP/honeycomb composite sandwich panels. *Thin-walled Struct.* 2021;169:108279.
 - [35] Zhang Y, Liu Q, He Z, Zong Z, Fang J. Dynamic impact response of aluminum honeycombs filled with Expanded Polypropylene foam. *Compos, Part B Eng.* 2019;156:17–27.
 - [36] Zhou H, Zhang X, Wang X, Wang Y, Zhao T. Response of foam concrete-filled aluminum honeycombs subject to quasistatic and dynamic compression. *Compos Struct.* 2020;239:112025.
 - [37] Shan J, Xu S, Zhou L, Wang D, Liu Y, Zhang M, et al. Dynamic fracture of aramid paper honeycomb subjected to impact loading. *Compos Struct.* 2019;223:110962.
 - [38] Wang Z, Gao G, Tian H, Lu Z. A stability maintenance method and experiments for multilayer tandem aluminum honeycomb array. *Int J Crashworthiness.* 2013;18(5):483e91.
 - [39] Liu Y, Zhou Q, Wei X, Xia Y. Testing and modeling tearing and air effect of aluminum honeycomb under out-of-plane impact loading. *Int J Impact Eng.* 2020;135:103402.
 - [40] Xing Y, Yang S, Li Z, Lu S, Zhang P, An Y, et al. Simulation and application of Bi-directional corrugated honeycomb aluminum as filling material for impact limiter of nuclear spent fuel transport cask. *Nucl Eng Des.* 2020;361:110502.
 - [41] Warren J, Cole M, Offenberger S, Kota KR, Lacy TE, Toghiani H, et al. Hypervelocity Impacts on Honeycomb Core Sandwich

- Panels Filled with Shear Thickening Fluid. *Int J Impact Eng.* 2021;150:103803.
- [42] Li X, Lu F, Zhang Y, Lin Y, Meng Y. Experimental study on out-of-plane mechanical and energy absorption properties of combined hexagonal aluminum honeycombs under dynamic impact. *Mater Des.* 2020;194:108900.
- [43] Onsalung N, Thinvongpituk C, Pianthong K. Impact Response of Circular Aluminum Tube Filled with Polyurethane Foam. *Mater Trans.* 2014;55(1):207–15.
- [44] Junchuan V, Thinvongpituk C. The Influence of Fiber Orientation and Stacking Sequence on the Crush Behavior of Hybrid AL/GFRP Tubes under Axial Impact. *Mater Trans.* 2020;61(7):1322–31.
- [45] Sakkampang K, Thinvongpituk C. The study on application of rubber sponges for impact absorber for motorcycle helmets [IJMPE]. *Int J Mech Prod Eng.* 2020;8(3):52–7.
- [46] Zhang Y, Yan L, Zhang C, Guo S. Low-velocity impact response of tube-reinforced honeycomb sandwich structure. *Thin-walled Struct.* 2021;158:107188.
- [47] Pratomo AN, Santosa SP, Gunawan L, Widagdo D, Putra IS. Numerical study and experimental validation of blastworthy structure using aluminum foam sandwich subjected to fragmented 8 kg TNT blast loading. *Int J Impact Eng.* 2020;146:103699.
- [48] Hao P, Du J. Energy absorption characteristics of bio-inspired honeycomb column thin-walled structure under impact loading. *J Mech Behav Biomed Mater.* 2018;79:301–8.
- [49] Dong Z, Shen L, Wei K, Wang Z. Compressive behaviors of fractal-like honeycombs with different array configurations under low velocity impact loading. *Thin-walled Struct.* 2021;163:107759.
- [50] Xie S, Zhou H. Analysis and optimisation of parameters influencing the out-of-plane energy absorption of an aluminium honeycomb. *Thin-walled Struct.* 2015;89:169–77.
- [51] Zhang Y, Li Y, Guo K, Zhu L. Dynamic mechanical behaviour and energy absorption of aluminium honeycomb sandwich panels under repeated impact loads. *Ocean Eng.* 2021;219:108344.
- [52] Qi J, Li C, Tie Y, Zheng Y, Duan Y. Energy absorption characteristics of origami-inspired honeycomb sandwich structures under low-velocity impact loading. *Mater Des.* 2021;207:109837.